THE JOURNAL OF BIOLOGICAL CHEMISTRY VOL. 282, NO. 31, pp. 22662–22667, August 3, 2007

The Role of the Poly(ADP-ribose) Polymerase Tankyrase1 in Telomere Length Control by the TRF1 Component of the Shelterin Complex*

Received for publication, March 27, 2007, and in revised form, June 8, 2007 Published, JBC Papers in Press, June 8, 2007, DOI 10.1074/jbc.M702620200

Jill R. Donigian[1] **and Titia de Lange**[2]

From the Laboratory of Cell Biology and Genetics, The Rockefeller University, New York, New York 10021

Tankyrase1 is a multifunctional poly(ADP-ribose) polymerase that can localize to telomeres through its interaction with the shelterin component TRF1. Tankyrase1 poly(ADP-ribosyl)ates TRF1 *in vitro*, and its nuclear overexpression leads to loss of TRF1 and telomere elongation, suggesting that tankyrase1 is a positive regulator of telomere length. In agreement with this proposal, we show that tankyrase1 RNA interference results in telomere shortening proportional to the level of knockdown. Furthermore, we show that a tankyrase1-resistant form of TRF1 enforced normal telomere length control, indicating that tankyrase1 is not required downstream of TRF1 in this pathway. Thus, in human cells, tankyrase1 appears to act upstream of TRF1, promoting telomere elongation through the removal of TRF1. This pathway appears absent from mouse cells. We show that murine TRF1, which lacks the canonical tankyrase1-binding site, is not a substrate for tankyrase1 poly(ADP-ribosyl)sylation *in vitro*. Furthermore, overexpression of tankyrase1 in mouse nuclei did not remove TRF1 from telomeres and had no detectable effect on other components of mouse shelterin. We propose that the tankyrase1-controlled telomere extension is a human-specific elaboration that allows additional control over telomere length in telomerase positive cells.

Telomeres can be elongated by the telomere-specific reverse transcriptase telomerase and shortened through the effects of DNA replication and nucleolytic attack. The TTAGGG repeat array of vertebrate telomeres has a species-specific length setting, suggesting that these forces are balanced in the germ line. Telomere length control has been primarily studied in human tumor cells that express telomerase (reviewed in Ref. 1). Such cells often maintain the length of their telomeres within a set range. This telomere length homeostasis is achieved through a negative feedback loop involving shelterin, the telomere-specific protein complex (2). Shelterin is comprised of six proteins (TRF1, TRF2, POT1, TPP1, TIN2, and Rap1) whose abundance at chromosome ends is dictated by the length of the duplex telomeric repeat array. All shelterin components behave as negative regulators of telomere elongation by telomerase. Inhibition of TRF1, TPP1, TIN2, and POT1 results in telomere elongation, whereas overexpression of several shelterin components shortens the length of the telomeres. Telomere healing experiments demonstrated that cells have the ability to monitor and regulate telomerase at individual telomeres, and tethering of TRF1 at subtelomeric sites showed that TRF1 can modulate telomere length in cis. These findings have resulted in a model for shelterin-dependent telomere length homeostasis whereby long telomeres contain more shelterin and thus have a diminished chance of being elongated further by telomerase. A key player in this negative feedback loop is POT1, whose binding to the single-stranded telomeric DNA appears to block telomerase *in vivo* (3–5) and *in vitro* (6–9).

The length of human telomeres can be reset by manipulating tankyrase1 (TRF1-interacting ankyrin related ADP-ribose polymerase), a PARP[3] with a diverse set of targets in different subcellular compartments (10–18). Although tankyrase1 is not a core component of shelterin, it can bind to a short motif in the N-terminal acidic domain of TRF1 (12) and PARsylates TRF1 *in vitro*, inhibiting its ability to bind to telomeric DNA (13). Upon overexpression of tankyrase1 in the nucleus, TRF1 is removed from telomeres and degraded by ubiquitin-mediated proteolysis (13, 14). Concomitant with the loss of TRF1, such cells display a telomere elongation phenotype that requires the catalytic activity of the PARP domain of tankyrase1 (15–18). TRF1 can be protected from the effect of tankyrase1 by TIN2, which forms a ternary complex with tankyrase1 and TRF1 and blocks the PARsylation of TRF1 *in vitro* (18). When TIN2 is inhibited *in vivo*, TRF1 appears more sensitive to the endogenous tankyrase1, and telomere elongation occurs.

Collectively, these results implicate tankyrase1 as a positive regulator of telomere elongation by telomerase. Several approaches have been used to provide further evidence for such a role of endogenous tankyrase1. PARP inhibitors were shown to induce telomere shortening, but it has been difficult to ascribe this phenotype to inhibition of tankyrase1 rather than one of the other PARPs (16). Dominant negative alleles of

* This work was supported by NCI National Institutes of Health Grant CA076027 (to T. d. L.). The costs of publication of this article were defrayed in part by the payment of page charges. This article must therefore be hereby marked "*advertisement*" in accordance with 18 U.S.C. Section 1734 solely to indicate this fact.

[1] Supported by a T32 training grant in support of the Rockefeller University Graduate Program (Grant T32 CA0096673).

[2] To whom correspondence should be addressed: The Rockefeller University, Box 159, 1230 York Ave., New York, NY 10021. Tel.: 212-327-8146; Fax: 212-327-7147; E-mail: delange@mail.rockefeller.edu.

[3] The abbreviations used are: PARP, poly(ADP-ribose) polymerase; PARsylate, poly(ADP-ribosyl)ate; shRNA, short hairpin RNA; PBS, phosphate-buffered saline; MEF, mouse embryonic fibroblast; h, human; m, mouse; PD, population doubling.

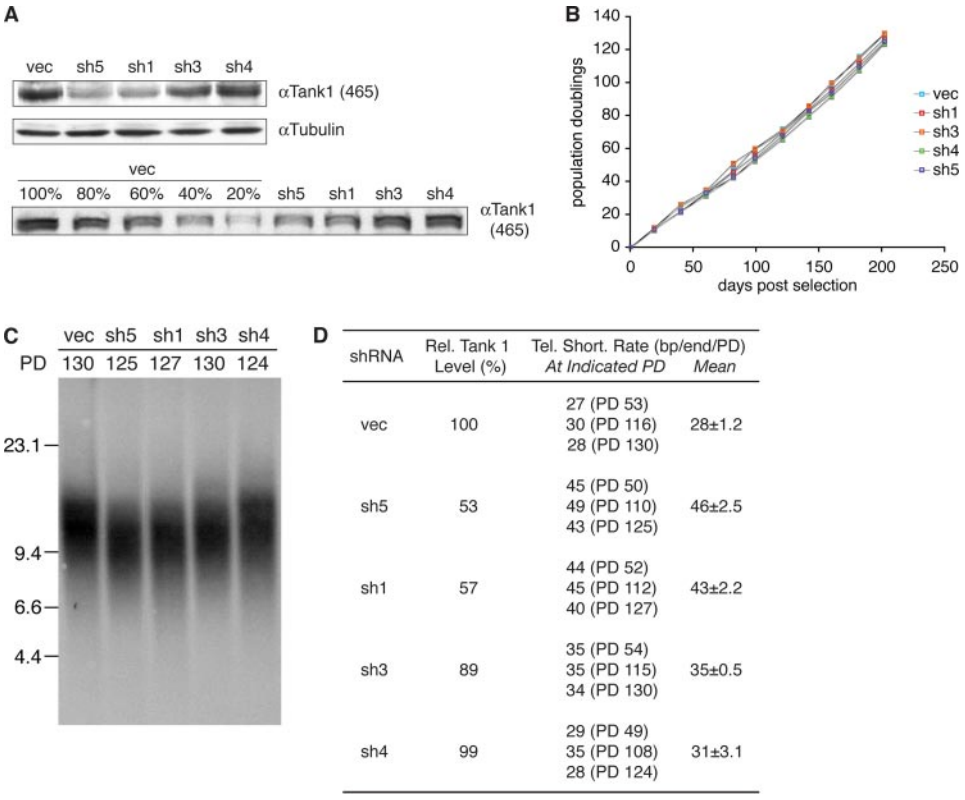

FIGURE 1. **Tankyrase1 suppression causes telomere shortening.** *A*, Western blots showing tankyrase1 protein levels in BJ-hTERT cells expressing shRNA-encoding retroviruses and the vector control (*vec*). Total cellular proteins were analyzed by immunoblotting using antibodies to tankyrase1 (465) (*αTank1*) and to γ-tubulin (*αTubulin*). *B*, graph of growth curves of BJ-hTERT cells infected with tankyrase1 shRNAs and the vector control. Cells were selected with puromycin for 5 days, and then proliferation was monitored over several months. *C*, genomic blot of telomeric restriction fragments in four BJ-hTERT cell lines infected with the indicated tankyrase1 shRNA retroviruses and the vector control. DNA agarose plugs were prepared at ~PD 130, digested with AluI and MboI, and analyzed by Southern blotting using a double-stranded TTAGGG repeat probe. *D*, table summarizing the relative (*Rel.*) tankyrase1 protein levels and the telomere (*Tel. Short.*) shortening rates of BJ-hTERT cells expressing tankyrase1 shRNAs.

tankyrase1 have largely failed to yield the expected telomere shortening phenotypes (15, 17), although success with one allele has been reported (16). Here we address this issue further by examining the telomere dynamics of cells targeted with tankyrase1 shRNAs and through the use of a tankyrase1-resistant allele of TRF1.

EXPERIMENTAL PROCEDURES

Tankyrase1 shRNA and Telomere Length Analysis—We generated four tankyrase1 shRNAs in pSUPER-retro (OligoEngine) and performed retroviral infections in BJ-hTERT cells as described previously (19). The sequences of the shRNA targets are as follows: sh1, 5′-GGCAGTGGCAGTAACAATT-3′; sh3, 5′-GAGGTTGTGAGTCTGTTAT-3′; sh4, 5′-GCGCTGATCCTACGTTAGT-3′; sh5, 5′-GCGTCGCTCTCAGCATCAT-3′. Total cellular proteins were analyzed by immunoblotting using antibodies to tankyrase1 (465), and the relative tankyrase1 protein levels were quantified by densitometry using the AlphaImager 2200 program (Alpha Innotech). For telomere length analysis, the cells were harvested, made into DNA agarose plugs, digested with AluI and MboI, separated on a 0.6% agarose gel, and transferred to a Hybond membrane for hybridization using an 800-bp telomeric DNA probe from pSP73Sty11 labeled by Klenow fragment and [α-^{32}P]dCTP. We exposed the blot to a PhosphorImager screen and quantified telomeric DNA signals using ImageQuant. The rates of telomere shortening were calculated by linear regression.

Generation of hTRF1$^{\Delta Tank}$—hTRF1$^{\Delta Tank}$ (hTRF1R13A/G14R) was made in the Gateway pENTR vector (Invitrogen) using the Stratagene QuikChange site-directed mutagenesis kit according to the manufacturer's instructions. A Clonase reaction was performed to transfer hTRF1$^{\Delta Tank}$ to the following destination vectors: pDEST14 for *in vitro* translation, pLPC MYC for 293T transfection and for retroviral infection, and pDEST10 for baculovirus production.

Far Western Analysis—Far Western assays were carried out as described previously (20) Two micrograms of purified protein derived from insect cells were subjected to SDS-PAGE and then blotted onto nitrocellulose. The blots were incubated in blocking buffer (10 mM HEPES (pH 7.5), 50 mM NaCl, 10 mM $MgCl_2$, 0.1 mM EDTA, 1 mM dithiothreitol, 10% glycerol, and 5% milk) for 3 h at 4 °C. Following the blocking step, the blots were probed overnight at 4 °C with ^{35}S-labeled *in vitro* translated protein prepared using the TNT T7-coupled reticulocyte lysate system (Promega) (a 50-μl reaction mixture in 5 ml of blocking buffer). The next morning, the blots were washed five times every 30 min in wash buffer (10 mM HEPES (pH 7.5), 50 mM NaCl, 10 mM $MgCl_2$, 0.1 mM EDTA, 1 mM dithiothreitol, 10% glycerol, and 0.25% milk) and then incubated with Amplify (Amersham Biosciences) for 10 min. The blots were exposed on a PhosphorImager screen overnight.

Transfection and Immunoprecipitation—293T cell transfection and immunoprecipitation was done as described previously (18). We plated human 293T cells (5–6 × 10^6) and transfected them 20–24 h later by the calcium phosphate co-precipitation method using 10–20 μg of plasmid DNA per 10 cm dish. We changed the medium after 12 h and collected cells 24–30 h after transfection. For immunoprecipitations, we dislodged 293T cells from the dish by flushing with cold phosphate-buffered saline (PBS), collected them by centrifugation, and lysed them in ice-cold buffer (50 mM Tris-HCl (pH 7.4), 1 mM EDTA, 400 mM NaCl, 1% Triton X-100, 0.1% SDS, 1 mM dithiothreitol, 1 mM phenylmethylsulfonyl fluoride, and a protease inhibitor mixture). After 10 min on ice, we added an equal volume of ice-cold water and mixed thoroughly. The lysate was

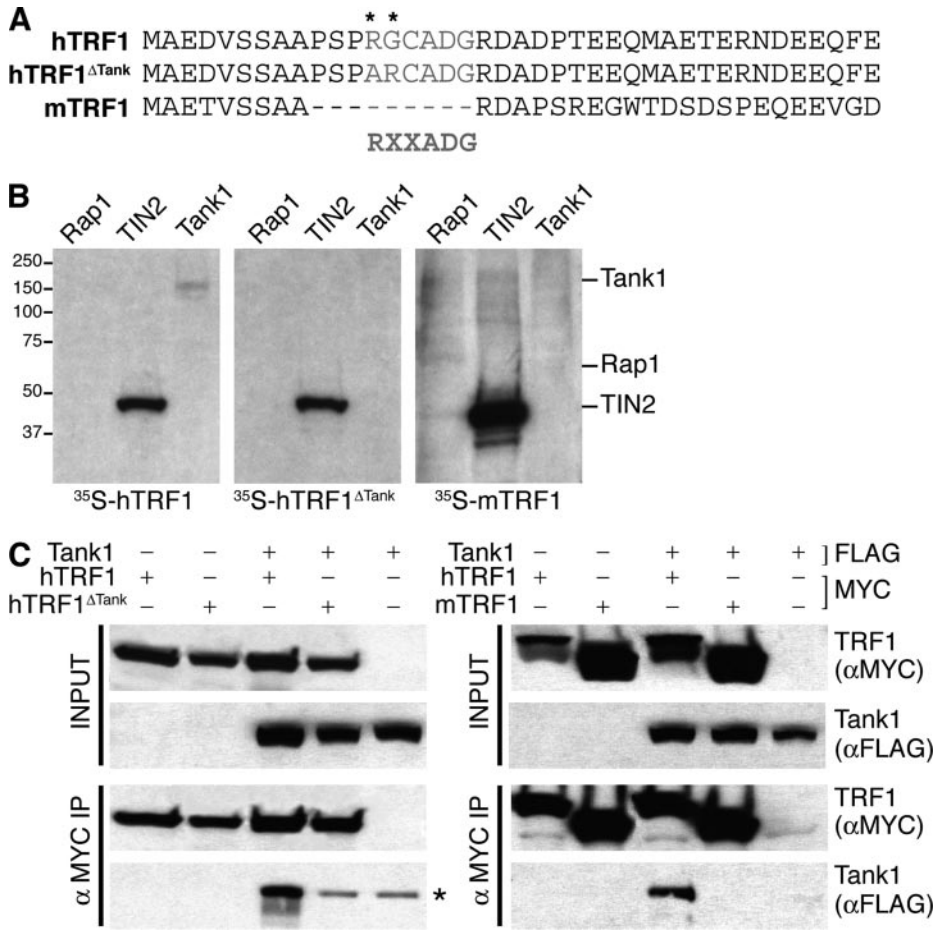

FIGURE 2. **hTRF1$^{\Delta Tank}$ and mTRF1 do not bind tankyrase1.** *A*, alignment of the N-terminal acidic domain of hTRF1, hTRF1$^{\Delta Tank}$, and mTRF1. The TRF1 tankyrase1-binding consensus sequence is also shown. *B*, far Western analysis of the tankyrase1 (*Tank1*) binding ability of hTRF1, hTRF1$^{\Delta Tank}$, and mTRF1. Each lane contains 2 μg of purified recombinant protein derived from insect cells using a His tag. The proteins were subjected to SDS-PAGE, blotted onto nitrocellulose, and incubated with the indicated ^{35}S-labeled *in vitro* translated protein. *C*, co-immunoprecipitations from transfected 293T cells. MYC-tagged hTRF1, hTRF1$^{\Delta Tank}$, mTRF1, and FN-tankyrase1 were transiently transfected into 293T cells in the combinations shown. Whole-cell extracts (*INPUT*) were immunoprecipitated (*IP*) using an antibody to MYC (9E10). A small fraction of FN-tankyrase1 is recovered nonspecifically in the immunoprecipitations resulting in the band indicated with an *asterisk*.

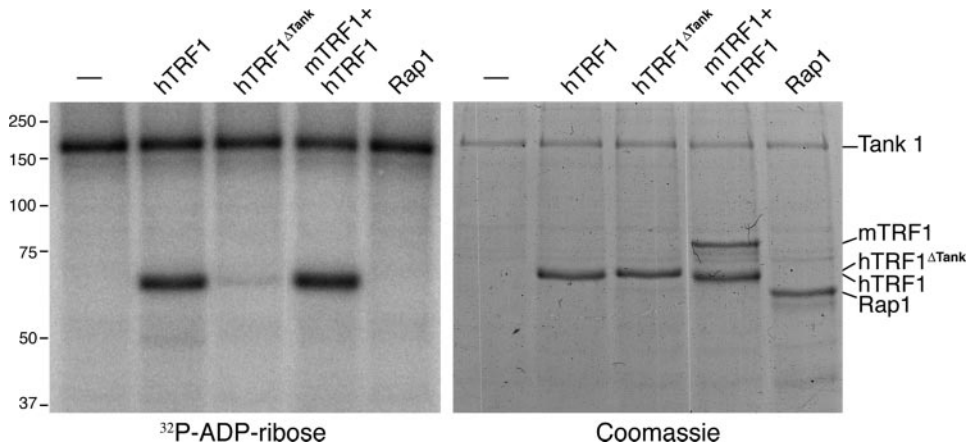

FIGURE 3. **hTRF1$^{\Delta Tank}$ and mTRF1 are not readily PARsylated by tankyrase1 (*Tank1*).** The autoradiograph (*left*) and Coomassie Blue-stained gel (*right*) from a tankyrase1 PARP assay. Each lane contains 4 μg of the indicated proteins derived from insect cells or *E. coli* cells (GST-mTRF1) in a reaction with [^{32}P]β-NAD$^+$. Products from each reaction were subjected to SDS-PAGE and processed for autoradiography or Coomassie Blue staining. The blot shown here yielded a hTRF1$^{\Delta Tank}$ signal that was 12% of the band intensity of wild type hTRF1.

centrifuged at 14,000 rpm for 10 min, and the supernatant was used for immunoprecipitation. The prepared lysates were incubated with 1 μg of MYC 9E10 mouse monoclonal antibody for 5–6 h at 4 °C, nutating. During the final hour, we added 30 μl (settled volume) of protein G-Sepharose beads (preblocked overnight with 10% bovine serum albumin in PBS) to each tube. We washed the beads three times with lysis buffer, eluted proteins with Laemmli loading buffer, and analyzed them by SDS-PAGE.

In Vitro PARP Assay—The *in vitro* tankyrase1 PARP assay was performed as described (13) with slight modifications. We incubated 4 μg of proteins purified from baculovirus-infected insect cells or *Escherichia coli* cells (GST-mTRF1) with [^{32}P]β-NAD$^+$ (1.3 μM) at 25 °C for 30 min. The reactions were stopped by adding ice-cold trichloroacetic acid to 25%. After 10 min on ice, we collected proteins by microcentrifugation (10 min at 14,000 rpm at 4 °C). The pellets were rinsed gently with ice-cold 5% trichloroacetic acid and dissolved in sample loading buffer (1 M Tris-base, 12% SDS, 0.2 M dithiothreitol, and 0.1% bromphenol blue). We separated the samples by SDS-PAGE and analyzed them by autoradiography and Coomassie Blue staining.

Transient Transfection and Indirect Immunofluorescence—FLAG-NLS-tagged tankyrase1 (FN-tankyrase1) was transfected into HeLa1.2.11 cells using Lipofectamine 2000 (Invitrogen) or into NIH 3T3 cells and MEFs by nucleofection (Amaxa) according to the manufacturer's protocol. Cells were fixed 48 h after transfection for 10 min at room temperature with PBS containing 2% paraformaldehyde and permeabilized for 10 min in PBS containing 0.5% Nonidet P-40. Nonspecific interactions were blocked by incubation for 30 min in PBS with 0.2% cold water fish gelatin and 0.5% bovine serum albumin (PBG). Thereafter, cells were incubated with primary antibody for 2 h at

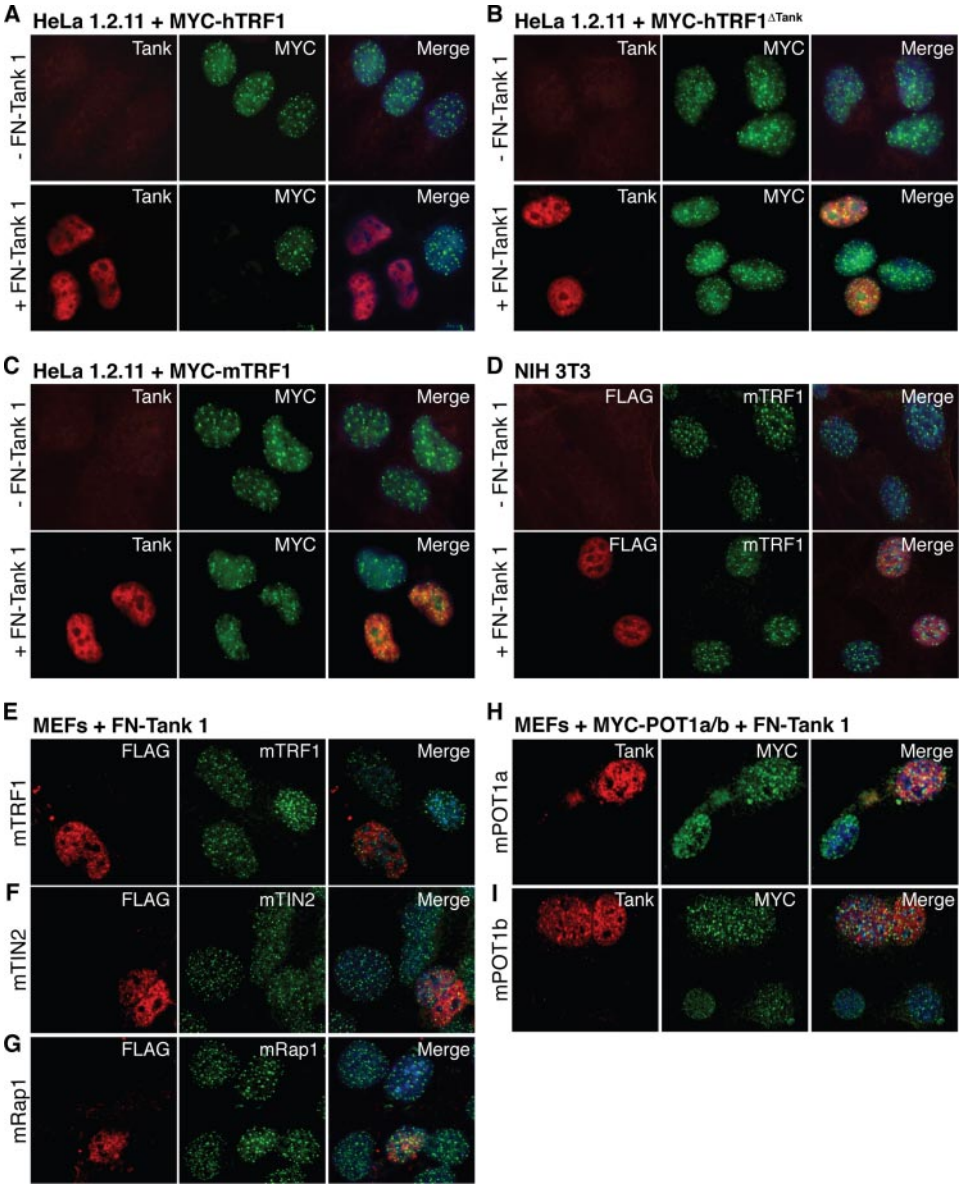

FIGURE 4. **Overexpression of tankyrase1 (*Tank*) in the nucleus releases hTRF1, but not hTRF1$^{\Delta Tank}$, mTRF1, or other mouse shelterin proteins.** *A–C*, indirect immunofluorescence of TRF1 localization as follows: HeLa1.2.11 cells stably expressing MYC-hTRF1 (*A*), MYC-hTRF1$^{\Delta Tank}$ (*B*), or MYC-mTRF1 (*C*). *D*, mouse NIH 3T3 cells transiently transfected with FN-tankyrase1 or mock-transfected. *E–I*, indirect immunofluorescence of mouse shelterin proteins mTRF1 (*E*), mTIN2 (*F*), mRap1 (*G*), mPOT1a (*H*), and mPOT1b (*I*) in immortalized MEFs transiently transfected with FN-tankyrase1. For *H* and *I*, immortalized MEFs stably expressing MYC-mPOT1a and MYC-mPOT1b were used, respectively.

room temperature. The following antibodies were used: tankyrase1, 465; MYC 9E10 (Calbiochem); FLAG M2 (Sigma); mTRF1 644; mTIN2 1447;[4] and mRap1 1252 (21). Cells were washed three times for 5 min using PBG and incubated with rhodamine- or fluorescein-conjugated secondary antibodies in PBG (Jackson Laboratory, Bar Harbor, Maine). DNA was stained with 4,6-diamino-2-phenylindole.

RESULTS AND DISCUSSION

Tankyrase1 shRNAs Affect Telomerase-mediated Telomere Elongation—To further address the role of tankyrase1 as a positive regulator of telomere length, we examined the telomere length of cells treated with tankyrase1 shRNAs. Since tankyrase1 deficiency is known to induce a mitotic arrest (22, 23) and thus would be incompatible with long term culturing, we aimed for shRNAs that would generate partial knockdown. We tested shRNAs for the residual tankyrase1 protein levels by quantitative Western blotting (Fig. 1, *A* and *D*) and identified two shRNAs that lowered the tankyrase1 level about 2-fold. A third shRNA had a very modest effect, and a fourth shRNA did not affect tankyrase1 and served as a control. None of these shRNAs affected the proliferation of the cells (Fig. 1*B*).

Since the knockdown of tankyrase1 is partial, we anticipated that its effect would be most easily monitored under conditions where telomerase is not in excess since high levels of telomerase can mask regulatory pathways (24). Our BJ-hTERT cells showed gradual telomere shortening despite the fact they are expressing telomerase. Their shortening rate was 25–30 bp/end/PD, which is significantly less than for telomerase-negative BJ cells (80 bp/end/PD) (19), indicating that telomerase is active at a significant but low level. If tankyrase1 contributes to the telomerase pathway in these cells, we would expect to detect an increase in the shortening rate from 25–30 bp/end/PD to the maximal rate of 80 bp/end/PD. To be able to determine such changes accurately, BJ-hTERT cells expressing the various shRNAs were cultured in parallel with the vector control for ~130 PDs, and the telomere shortening rates were determined based on multiple genomic blots at various PDs (Fig. 1, *C* and *D*). The results indicated that tankyrase1 shRNAs sh1 and sh5 resulted in a significant increase in the shortening rate to 43 ± 2.2 and 46 ± 2.5 bp/end/PD, respectively. The less effective sh3 had a minor effect (shortening at 35 ± 0.5 bp/end/PD), and as expected, cells expressing the ineffective sh4 had a similar shortening rate as the vector control cells (31 ± 3.1 bp/end/PD). Together with previous data indicating that tankyrase1 does not affect telomere dynamics in telomerase-negative cells (15), our results confirm the role for tankyrase1 as a positive regulator of the telomerase pathway.

Mutation of the Tankyrase1-binding Motif of TRF1—In the simplest model for the effect of tankyrase1 on telomere main-

[4] J. R. Donigian and T. de Lange, unpublished data.

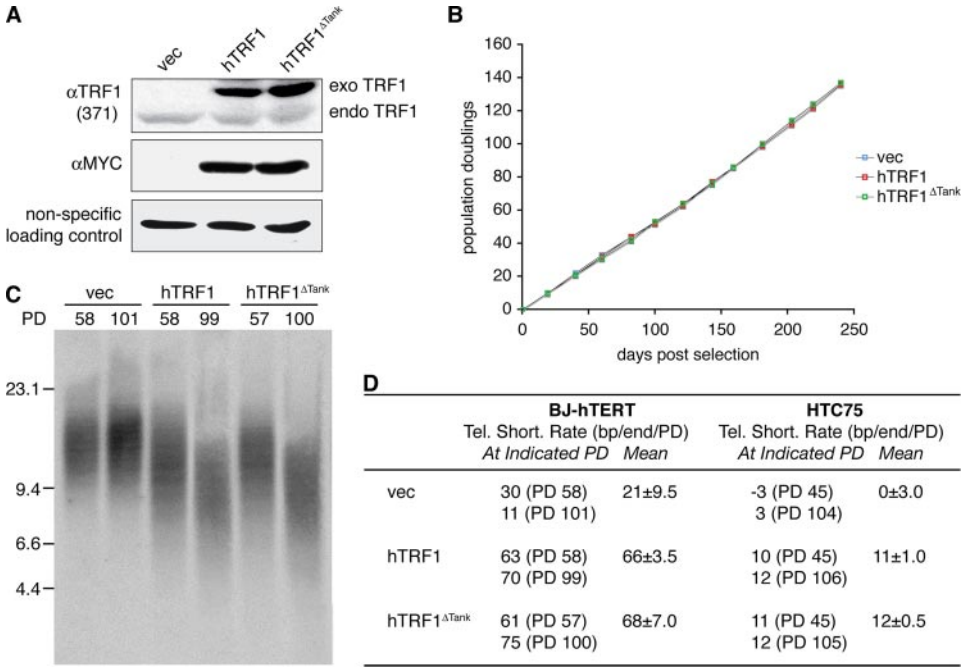

D

	BJ-hTERT Tel. Short. Rate (bp/end/PD) At Indicated PD	Mean	HTC75 Tel. Short. Rate (bp/end/PD) At Indicated PD	Mean
vec	30 (PD 58) 11 (PD 101)	21±9.5	-3 (PD 45) 3 (PD 104)	0±3.0
hTRF1	63 (PD 58) 70 (PD 99)	66±3.5	10 (PD 45) 12 (PD 106)	11±1.0
hTRF1$^{\Delta Tank}$	61 (PD 57) 75 (PD 100)	68±7.0	11 (PD 45) 12 (PD 105)	12±0.5

FIGURE 5. **Overexpression of hTRF1$^{\Delta Tank}$ causes telomere shortening.** *A*, Western blots of endogenous (*endo*) TRF1 and exogenously (*exo*) expressed MYC-tagged hTRF1 and hTRF1$^{\Delta Tank}$ in BJ-hTERT cells. Total cellular proteins were analyzed by immunoblotting using antibodies to TRF1 (371), MYC (9E10), and γ-tubulin. *vec*, vector control. *B*, graph of growth curves of BJ-hTERT cells infected with hTRF1, hTRF1$^{\Delta Tank}$, and the vector control. Cells were selected with puromycin for 5 days, and then proliferation was monitored over 130 PDs. *C*, genomic blot of telomeric restriction fragments in BJ-hTERT cell lines infected with hTRF1 and hTRF1$^{\Delta Tank}$ retroviruses and the vector control. DNA agarose plugs were prepared at the indicated PDs, digested with AluI and MboI, and analyzed by Southern blotting using a TTAGGG repeat probe. *D*, table summarizing the telomere shortening (*Tel. Short.*) rates of BJ-hTERT and HTC75 cells expressing hTRF1, hTRF1$^{\Delta Tank}$, and the vector control.

tenance, the enzyme binds and PARsylates TRF1, removing TRF1 from telomeres. Here, tankyrase1 only acts upstream of TRF1 and is not required for the ability of TRF1 to function as a negative regulator of telomere length. However, the data do not exclude the possibility that tankyrase1 may also have a role downstream of TRF1, affecting the negative regulation of telomere length by TRF1 (18). To examine this possibility, we generated a TRF1 mutant that lacks a functional tankyrase1 interaction motif and determined whether it was still capable of negatively regulating telomere length. In characterizing the minimal tankyrase-binding motif, it was shown that the first residue in the hexapeptide R*XX*ADG is critical for tankyrase binding, whereas substitution of the second residue had no effect on binding (12). Using site-directed mutagenesis, a mutation was made in the N-terminal ^{13}RGCADG^{18} motif of hTRF1 by converting arginine 13 to an alanine (Fig. 2*A*). Additionally, glycine 14 was inadvertently mutated to an arginine. The ability of this hTRF1$^{\Delta Tank}$ protein to bind tankyrase1 was tested by far Western assay. Baculovirus-derived TIN2, tankyrase1, and Rap1 (as a negative control) were probed with *in vitro* translated ^{35}S-labeled hTRF1 and hTRF1$^{\Delta Tank}$. The results showed that wild type hTRF1 was able to bind tankyrase1, whereas hTRF1$^{\Delta Tank}$ failed to do so. On the other hand, the mutation did not affect the TRF1-TIN2 association, as demonstrated by the robust signal in the TIN2 lane for both wild type hTRF1 and the mutant (Fig. 2*B*). Co-immunoprecipitation experiments also indicated that hTRF1$^{\Delta Tank}$ no longer bound tankyrase1. MYC-tagged hTRF1 and hTRF1$^{\Delta Tank}$ were transiently co-transfected with FN-tankyrase1 into 293T cells, and TRF1 was precipitated from the cells using an antibody against MYC. The immunoblot shows that wild type hTRF1 was able to pull down tankyrase1, whereas hTRF1$^{\Delta Tank}$ failed to do so (Fig. 2*C*).

hTRF1$^{\Delta Tank}$ Is Resistant to Tankyrase1 Activity in Vitro and in Vivo—We next tested whether the hTRF1$^{\Delta Tank}$ mutant could be PARsylated by tankyrase1 in an *in vitro* PARP assay (Fig. 3). The PARsylation of hTRF1$^{\Delta Tank}$ by tankyrase1 was reduced by 4–5-fold when compared with wild type hTRF1 (22 ± 7.6% of wild type in three experiments). The discrepancy between the ability of hTRF1$^{\Delta Tank}$ to bind tankyrase1 and to be modified by tankyrase1 may lie in the sensitivity of the assays used. It is possible that hTRF1$^{\Delta Tank}$ can still loosely associate with tankyrase1 outside of its acidic domain (25), allowing for modest PARsylation of hTRF1$^{\Delta Tank}$. In fact, this is the case with chicken TRF1, which binds tankyrase1 although it lacks the R*XX*ADG tankyrase-binding motif (26).

Finally, we tested the ability of hTRF1$^{\Delta Tank}$ to resist removal from the telomere in the presence of excess nuclear tankyrase1 *in vivo*. HeLa cells expressing MYC-tagged hTRF1 or hTRF1$^{\Delta Tank}$ were transiently transfected with FN-tankyrase1, and the removal of TRF1 was monitored by indirect immunofluorescence. As expected, hTRF1 was no longer detectable at telomeres in the nuclei that expressed tankyrase1 (Fig. 4*A*). In contrast, hTRF1$^{\Delta Tank}$ retained its punctuate pattern in tankyrase1-expressing cells (Fig. 4*B*). We conclude that hTRF1$^{\Delta Tank}$ has largely lost tankyrase1 interaction *in vitro* and *in vivo*.

hTRF1$^{\Delta Tank}$ Behaves as a Negative Regulator of Telomere Length—To evaluate the effect of the diminished tankyrase1 interaction on the telomere length regulatory activity of TRF1, we analyzed telomere length in BJ-hTERT and HTC75 cells overexpressing wild type hTRF1 and hTRF1$^{\Delta Tank}$. Both proteins were expressed at the same level (Fig. 5*A*). Their overexpression was such that only ~15% of the total TRF1 in the cells was derived from the endogenous (wild type) locus. hTRF1$^{\Delta Tank}$ had no effect on the viability of the cells, and they proliferated at the same rate as cells expressing hTRF1 or the vector control (Fig. 5*B* and data not shown). As seen in the tankyrase1 shRNA experiment, the BJ-hTERT vector control cells experienced mild telomere shortening (21 ± 9.5 bp/end/PD), whereas the HTC75 vector control cells remained at a stable telomere length setting. Overexpression of hTRF1 led to telomere shortening at a rate of 66 ± 3.5 bp/end/PD in BJ-

hTERT cells and 11 ± 1.0 bp/end/PD in HTC75 cells (Fig. 5, *C* and *D*; data not shown). A similar shortening phenotype was evident for the cells expressing hTRF1$^{\Delta Tank}$, which induced a shortening rate of 68 ± 7.0 bp/end/PD in BJ-hTERT cells and 12 ± 0.5 bp/end/PD in HTC75 cells (Fig. 5, *C* and *D*; data not shown). This result implies that diminished recruitment of tankyrase1 does not have a strong impact on the ability of TRF1 to negatively regulate telomere length. Thus, tankyrase1 appears to primarily act upstream of TRF1 in the telomere length regulation pathway.

Mouse TRF1 Does Not Interact with Tankyrase1 in Vitro and in Vivo—Interestingly, the N terminus of mouse TRF1 lacks the RGCADG motif (Fig. 2*A*) and does not bind tankyrase1 (12). This would suggest that the wild type mTRF1 would resemble the hTRF1$^{\Delta Tank}$ mutant. To test this idea, we asked whether full-length mTRF1 could interact with and be modified by tankyrase1. Human and mouse tankyrase1 are 98% identical overall, with most differences occurring in the N terminus, which is not implicated in the interaction with TRF1 or its PARP activity. We therefore used the available human tankyrase1 constructs for these tests because this approach allowed comparison of human and mouse TRF1 in the same experiment. In the far Western assay, mTRF1 behaved similarly to hTRF1$^{\Delta Tank}$, forming a complex with TIN2 yet failing to interact with tankyrase1 (Fig. 2*B*). Furthermore, mTRF1 did not bind tankyrase1 based on their lack of co-immunoprecipitation from transfected 293T cells (Fig. 2*C*). Additionally, GST-mTRF1 was not PARsylated by tankyrase1 in an *in vitro* PARP assay (Fig. 3). The reaction was validated by showing that hTRF1 and tankyrase1 were still modified in the presence of GST-mTRF1. This control was included to rule out that GST-mTRF1, the only protein prepared from bacteria, did not contain a fortuitous inhibitor of the PARP reaction. The effect of tankyrase1 on mTRF1 telomere localization was also examined. HeLa 1.2.11 cells infected with MYC-mTRF1 (Fig. 4*C*), NIH 3T3 cells (Fig. 4*D*), and MEFs (Fig. 4*E*) were transfected with FN-tankyrase1, and the distribution of mTRF1 was assessed by immunofluorescence. As with hTRF1$^{\Delta Tank}$, tankyrase1 failed to remove mTRF1 from telomeres. We also examined the effect of nuclear overexpression of tankyrase1 on the telomeric localization of other shelterin components, including mTIN2 (Fig. 4*F*), mRap1 (Fig. 4*G*), mPOT1a (Fig. 4*H*), and mPOT1b (Fig. 4*E*). For none of these shelterin proteins was tankyrase1 found to affect their localization.

Collectively, the data suggest that tankyrase1 does not have the same role at mouse telomeres that is observed for human telomeres. This is not the first time a difference has been seen between human and mouse telomeres. The most striking recent divergence is the fact that rodent shelterin is comprised of two functionally distinct POT1 proteins, both of which are required to protect the telomere, whereas human shelterin only includes a single POT1 protein (27). Our data suggest that the use of tankyrase1 as a shelterin accessory factor is another example of the rapid evolution of the telomere/telomerase system. Tankyrase1 presumably provides an additional level of control over telomere elongation by telomerase. Perhaps the tankyrase1 pathway allows the subset of telomerase positive human somatic cells to control the rate of telomere shortening.

Acknowledgments—We thank Jeffrey Ye for guidance and advice, especially during the early stages of this project, Dirk Hockemeyer for the MYC-POT1a/b MEFs, and Kristina Hoke for helpful comments on this manuscript.

REFERENCES

1. Smogorzewska, A., and de Lange, T. (2004) *Ann. Rev. Biochem.* **73,** 177–208
2. de Lange, T. (2005) *Genes Dev.* **19,** 2100–2110
3. Liu, D., Safari, A., O'Connor, M. S., Chan, D. W., Laegeler, A., Qin, J., and Songyang, Z. (2004) *Nat. Cell. Biol.* **6,** 673–680
4. Loayza, D., and de Lange, T. (2003) *Nature* **424,** 1013–1018
5. Ye, J. Z., Hockemeyer, D., Krutchinsky, A. N., Loayza, D., Hooper, S. M., Chait, B. T., and de Lange, T. (2004) *Genes Dev.* **18,** 1649–1654
6. Kelleher, C., Kurth, I., and Lingner, J. (2005) *Mol. Cell. Biol.* **25,** 808–818
7. Lei, M., Zaug, A. J., Podell, E. R., and Cech, T. R. (2005) *J. Biol. Chem.* **280,** 20449–20456
8. Wang, F., Podell, E. R., Zaug, A. J., Yang, Y., Baciu, P., Cech, T. R., and Lei, M. (2007) *Nature* **445,** 506–510
9. Xin, H., Liu, D., Wan, M., Safari, A., Kim, H., Sun, W., O'Connor, M. S., and Songyang, Z. (2007) *Nature* **445,** 559–562
10. Chi, N. W., and Lodish, H. F. (2000) *J. Biol. Chem.* **275,** 38437–38444
11. Smith, S., and de Lange, T. (1999) *J. Cell Sci.* **112,** 3649–3656
12. Sbodio, J. I., and Chi, N. W. (2002) *J. Biol. Chem.* **277,** 31887–31892
13. Smith, S., Giriat, I., Schmitt, A., and de Lange, T. (1998) *Science* **282,** 1484–1487
14. Chang, W., Dynek, J. N., and Smith, S. (2003) *Genes Dev.* **17,** 1328–1333
15. Cook, B. D., Dynek, J. N., Chang, W., Shostak, G., and Smith, S. (2002) *Mol. Cell. Biol.* **22,** 332–342
16. Seimiya, H., Muramatsu, Y., Ohishi, T., and Tsuruo, T. (2005) *Cancer Cell* **7,** 25–37
17. Smith, S., and de Lange, T. (2000) *Curr. Biol.* **10,** 1299–1302
18. Ye, J. Z., and de Lange, T. (2004) *Nat. Genet.* **36,** 618–623
19. Karlseder, J., Smogorzewska, A., and de Lange, T. (2002) *Science* **295,** 2446–2449
20. Ye, J. Z., Donigian, J. R., Van Overbeek, M., Loayza, D., Luo, Y., Krutchinsky, A. N., Chait, B. T., and de Lange, T. (2004) *J. Biol. Chem.* **279,** 47264–47271
21. Celli, G., and de Lange, T. (2005) *Nat. Cell. Biol.* **7,** 712–718
22. Chang, P., Jacobson, M. K., and Mitchison, T. J. (2004) *Nature* **432,** 645–649
23. Dynek, J. N., and Smith, S. (2004) *Science* **304,** 97–100
24. Cristofari, G., and Lingner, J. (2006) *EMBO J.* **25,** 565–574
25. Seimiya, H., Muramatsu, Y., Smith, S., and Tsuruo, T. (2004) *Mol. Cell. Biol.* **24,** 1944–1955
26. De Rycker, M., Venkatesan, R. N., Wei, C., and Price, C. M. (2003) *Biochem. J.* **372,** 87–96
27. Hockemeyer, D., Daniels, J. P., Takai, H., and de Lange, T. (2006) *Cell* **126,** 63–77